



Emergent, linked traits of fluctuation feedback systemsZachary Jackson ^{*}*Department of Physics, University of Florida, Gainesville, Florida 32603, USA*Kurt Wiesenfeld *School of Physics, Georgia Institute of Technology, Atlanta, Georgia 30313, USA*

(Received 6 May 2021; accepted 13 December 2021; published 29 December 2021)

A variety of nonequilibrium systems display intermittent switching between semistable macroscopic behaviors. We identify a certain type of indeterminacy, with episodes of patterned behavior irregularly punctuated by transitions. It appears that the long-lived patterns are, not coincidentally, also low-fluctuation states. We describe these linked traits with a small set of examples.

DOI: [10.1103/PhysRevE.104.064216](https://doi.org/10.1103/PhysRevE.104.064216)**I. INTRODUCTION**

In equilibrium statistical mechanical systems, one can predict the long-term macroscopic properties even when the dynamics is a function of many degrees of freedom whose detailed motion is unknown. To do this, one assigns some probabilistic weighting to the state space and then averages over that state space. This approach is justified on the grounds that, because the number of microscopic bodies is large, the equilibrium values of macroscopic variables become prohibitively likely in the long-time limit.

Even in nonequilibrium settings, including cases where there are many degrees of freedom and/or complicated dynamics, systems may exhibit regular behavior. Often, this behavior is of a certain type. We mention here a diverse set of examples which motivate our thinking in what follows. A canonical example drawn from evolutionary science is the phenomenon of punctuated equilibrium, in which ecosystems exhibit long intervals of relatively stable population networks interrupted by short intervals of rapid speciation [1,2]. A similarly staccato dynamics can be seen in flux creep experiments on Type II superconductors where magnetic flux is expelled from the material in discrete “flux avalanche” events, widely varying in size, and occurring at irregular intervals. These represent the rapid rearrangement of current in the sample to a new steady state in response to a gradually ramped external field [3,4]. A third example is the emergence of coherent structures in turbulent fluid systems. In these systems there exist common spatial structures which live long enough to distinguish themselves from the surrounding disordered turbulent flow [5,6]. Lastly, consider recent active matter experiments on a so-called “supersmarticle” [7]. There, several simple self-actuated elements (called smarticles) placed in an anchored ring quickly find any one of a small number of nearly periodic patterns which persists for some time before breaking up; soon, a new one appears [8]. Some of these patterns are clear

to the eye; for a system of just three smarticles, some five or six recurrent patterns are observed, visited in apparently random order over the course of a single experimental run.

Each of the above examples is understood through the relevant biological, electromagnetic, mechanical, or dynamical system theories. Viewed broadly, however, their behaviors share a certain commonality, namely, the persistent recurrence of ordered but intermittent behavioral episodes. In this paper, we propose that this commonality of behavior can be understood in a general way: it arises from an inherent connection between the instantaneous degree of internal organization and the resulting effective fluctuation strength. If there is some portion of a system which can be considered organized and some portion which is not, the disorganized portion is the source of fluctuations. This means that the more of the system is in an organized state, the less is available as a source of effective noise.

We identify a class of systems (though we are unable to say how large this class may be) which display some uncertainty in their behavior but not so much so that the dynamical structure is totally washed out. These systems display a kind of intermittent behavior, showing episodes of mostly ordered dynamics, interrupted by shorter transitional intervals when disorder predominates. An intermediate timescale emerges over which the system is predictable in detail, although the long-term dynamics may only be characterized statistically. We illustrate this idea through a pair of complementary examples: a deterministic N -body metronome system and a modified version of the chaotic Lorenz equations. In the last section, we explicitly demonstrate the essential elements of this class of systems through a noise-driven double-well system. Finally, we consider how our results might connect to the recently developed notion of rattling [9,10].

The behavior we refer to here as intermittent is unrelated to the so-called type I, II, and III intermittency observed in systems with fixed parameters poised near a bifurcation [11,12]. In the systems we describe, intermittent behavior occurs robustly in that it does not require tuning a parameter close to a bifurcation and is natural in systems with many

^{*}zackljackson@ufl.edu

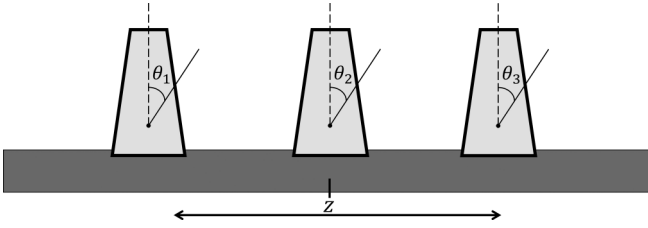


FIG. 1. Metronome setup. A cartoon of the coupled metronome system. θ_i is the deflection of the pendulum of metronome i from vertical. z is the position of the platform the metronomes are sitting on.

interacting parts. Our systems do not require any specific type of bifurcation, nor are they necessarily reducible to a low-dimensional state. Indeed, the high dimensionality is a feature which can allow random-like behavior even in the absence of chaos. What we identify is a mechanism for the emergence of intermittent behavior separate from the intermittency as developed using bifurcation analysis. We propose that this mechanism is common.

II. COUPLED METRONOMES

As a first example, consider a collection of N metronomes supported on a common mobile platform (see Fig. 1) [13]. We have in mind the case where N is reasonably large (say, of order 100). Each metronome has its own natural frequency, i.e., its frequency when uncoupled to the rest of the system. If the platform is held stationary, the metronomes are dynamically uncoupled, each metronome oscillates periodically, and the full system dynamics is N -frequency quasiperiodic. When the platform is free to move, the metronomes interact, and their motion tends to synchronize. For sufficiently large coupling (and/or sufficiently small disorder), the system can fully frequency lock, so that the system displays strictly periodic motion. In what follows, we want to consider the system somewhat below this fully synchronized threshold. Following Ref. [14], a set of nondimensional dynamical equations for the system is

$$\ddot{\theta}_i = -\frac{\omega_i}{\omega} \sin \theta_i - \frac{\beta}{\omega} \left[\left(\frac{\theta_i}{\theta_0} \right)^2 - 1 \right] \dot{\theta}_i - \frac{\omega_i^2}{g} \left(\frac{m}{M + Nm} \right) r_i \cos \theta_i \ddot{z}, \tag{1}$$

$$\ddot{z} = -\frac{1}{r} \sum_j^N r_j (\sin \theta_j), \tag{2}$$

where θ_i is the deflection of the i th pendulum, ω_i is its natural frequency, r_i is the distance from a metronome’s pivot to its center of mass, and z is the position of the platform. The r_i are chosen from a narrow uniform distribution around the mean $r = 0.05$. The platform has mass M and the pendulum masses m are identical. Finally, ω is the mean natural frequency.

The van der Pol term in Eq. (1) models the escapement, which drives the metronome when its phase is close to zero and damps its motion at large θ to prevent it from overturning. The parameter β controls the strength of this driving or

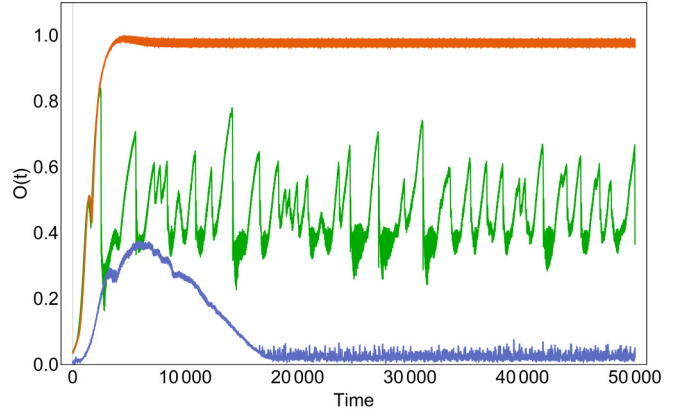


FIG. 2. Order parameter. The value of the normalized maximum Fourier amplitude vs time for different spreads of natural frequencies. Each set of frequencies is chosen by picking the arm lengths r_i from a uniform distribution within a fixed Δr about $r = 0.05$. The three traces correspond to $\Delta r = 0.003$ (orange), 0.015 (green), and 0.03 (blue).

dissipation. In our simulations, $N = 32$, $m = 0.1$, $M = 0.5$, $\beta = 0.01$, and $\theta_0 = \pi/16$.

The system behavior depends on the spread of natural frequencies and the mass of the platform. When the natural frequencies are sufficiently close together and the platform is light, the metronomes become synchronized: they are frequency locked, all of the metronome phases move together, and the platform moves back and forth periodically with large amplitude. In contrast, when the natural frequencies have a large spread the metronomes cannot synchronize, and they all move more or less at their own frequencies. This in turn causes the motion of the platform to be an erratic superposition of oscillations. For an intermediate spread of natural frequencies the system shows indeterminacy, as seen in the green trace in Fig. 2. For a while the metronomes are partially synchronized and the platform moves similarly to the synchronized case but with smaller amplitude. Episodically, the metronome with the smallest frequency gradually lags falls behind the others and stabilizes at twice the amplitude and twice the period as the rest.

These different behaviors are readily distinguishable using a well-chosen order parameter $O(t)$. For this purpose, we use the largest Fourier amplitude of the motion of the platform normalized so that the maximum possible value is 1. Symbolically, $O(t) = \text{Max}(\mathcal{F}[z](t))/P$. When the metronomes are unsynchronized the platform motion is the superposition of many frequencies, and the Fourier spectrum is flat. When the metronomes move together, the platform motion is nearly periodic, so its power is concentrated at one frequency. In practice, we take the discrete Fourier transform of $z(t)$ in a moving time window of length 25 time units with resolution 0.1 time units and take the magnitude of the maximum amplitude over all possible frequencies in that window normalized by the maximum value P of $\mathcal{F}[z](t)$ when all metronomes have identical natural frequencies. A time series of the order parameter for different spreads of natural frequencies is shown in Fig. 2.

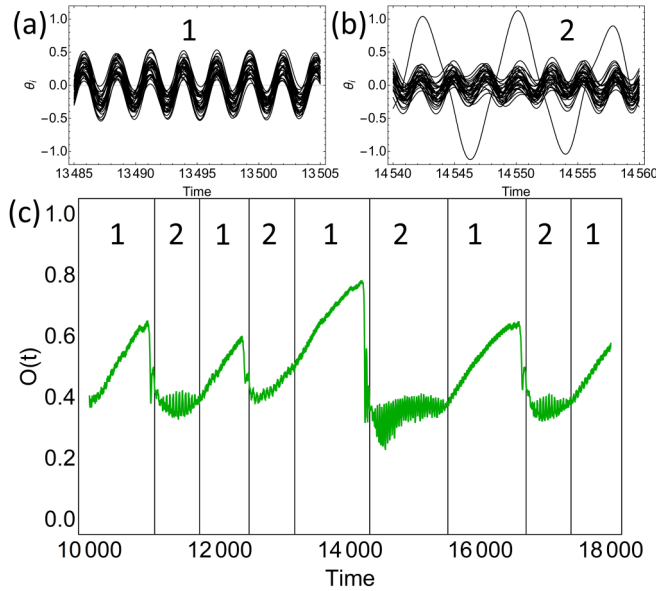


FIG. 3. Behavior and parameter detail. The two different identifiable behaviors of the metronome system with intermediate natural frequency spread. (a) Detailed look at pattern 1, where the metronomes are all moving together in a partially synchronized state. (b) Detailed look at pattern 2, where one metronome has a larger amplitude and period than the others. (c) A zoomed-in look at the order parameter time series from Fig. 2 with the two episodic behaviors identified.

The partially ordered regime deserves a closer look. A typical example is shown in Fig. 3. There are two distinct behaviors that the system exhibits during a single long run. Fundamentally, the governing dynamical equations are deterministic: there is no random noise to kick the system from one “state” to the other. Rather, the fluctuations arise as a result of the spread in natural frequencies. Because these frequencies are too spread out for the metronomes to exactly mutually frequency lock, the motion of the platform is to some degree irregular, and this motion feeds back to create an effective noise in the dynamics of each oscillator. It is this noise that kicks the system back and forth between two patterns of behavior. Occasionally, the system becomes substantially synchronized, the platform motion becomes fairly regular, and so the effective noise feedback is greatly reduced: this low-fluctuation epoch is self-consistently maintained.

A primary feature of this regime is the emergence of an intermediate timescale, namely, the *switching time* between persistent dynamical states.

III. MODIFIED LORENZ EQUATIONS

As our second example, we consider a modified version of the Lorenz equations [15], where feedback induces slow variations in a parameter. We take as governing equations

$$\dot{x} = \sigma(y - x), \quad (3)$$

$$\dot{y} = x(\rho - z) - y, \quad (4)$$

$$\dot{z} = xy - \beta, \quad (5)$$

$$\dot{\rho} = \delta x. \quad (6)$$

The first three equations are the original Lorenz system. Our modification makes ρ a variable rather than a parameter. As modified, this system provides an interesting complement to the metronome array because the Lorenz system has far fewer degrees of freedom but it can display complex behavior due to its chaotic dynamics. The behavior of the Lorenz equations is most familiar for the parameter values Lorenz focused on in his original paper, $(\sigma, \beta, \rho) = (10, 8/3, 28)$ [15]. In what follows, we set σ and β to these values, and let ρ evolve according to Eq. (6). The parameter $\delta = 0.1$ is small enough that the parameter turned variable ρ is slowly varying compared the x , y , and z . To understand the observed dynamics, it will be helpful to summarize the behavior of the (unmodified) Lorenz system [only Eqs. (3)–(5)] for different values of fixed ρ . Our summary is adapted from [16].

There are in general three fixed points: the origin and (for $\rho > 1$) two symmetrically located points C_1 and C_2 . For $\rho > 24.7\dots$, all three fixed points are unstable and the system is chaotic, except for certain parameter windows. In the chaotic regime the attractor has the familiar butterfly shape shown in Fig. 4 ($\rho = 25$). The trajectory spirals around C_1 and C_2 , switching lobes in a seemingly random manner. The distribution of possible numbers of orbits before switching lobes varies with ρ . For instance, when $\rho = 28$ the maximum number of consecutive revolutions on one side is 24. The trajectories get even more limited in the vicinity of a small number of period doubling windows. (These windows show an inverse period doubling cascade as ρ increases.) There is a narrow window near $\rho = 100$, another narrow window near $\rho = 150$, and a third that starts from near $\rho = 200$ and continues for arbitrarily large ρ . At the upper end of the period doubling window between $\rho = 99.524$ and $\rho = 100.795$ there are two stable periodic orbits, each consisting of two trips around one of the stationary points and one around the other. At the period doubling window near $\rho = 150$ the same phenomenon occurs, but the stable periodic orbits at the upper end of that window are a pair of figure eights looping around each of C_1 and C_2 only once before switching lobes.

Turning now to the modified system [Eqs. (3)–(6)], we distinguish between the slow parameter turned variable ρ and the fast variables x , y , z . Due to the feedback between Eq. (6) and Eq. (4), the slow variable dictates the distribution of trajectories of the fast variables and vice versa. Numerical simulations reveal that as the dynamics evolves, there are instances where the slow variable seems to stall, even though the system is not close to a fixed point. Typical results are shown in Fig. 5. The underlying mechanism for the stalling behavior can be found by viewing the fast dynamics as an effective noise source driving the slow variable ρ . On the one hand, the long-term average drift from the (deterministic) motion of x is zero because the average value of x is zero over long times for all values of ρ . Nevertheless, since the magnitude of the effective noise from x is inhomogeneous, the velocity of x in either direction is reduced in low noise-amplitude regions, causing x to preferentially dwell in these regions. The particular choice for Eq. (6) is motivated by having zero average drift, but this choice is not unique. We could have chosen any odd function of x or y .

To examine the stalling behavior more closely, we go back to the original (unmodified) Lorenz system and track the

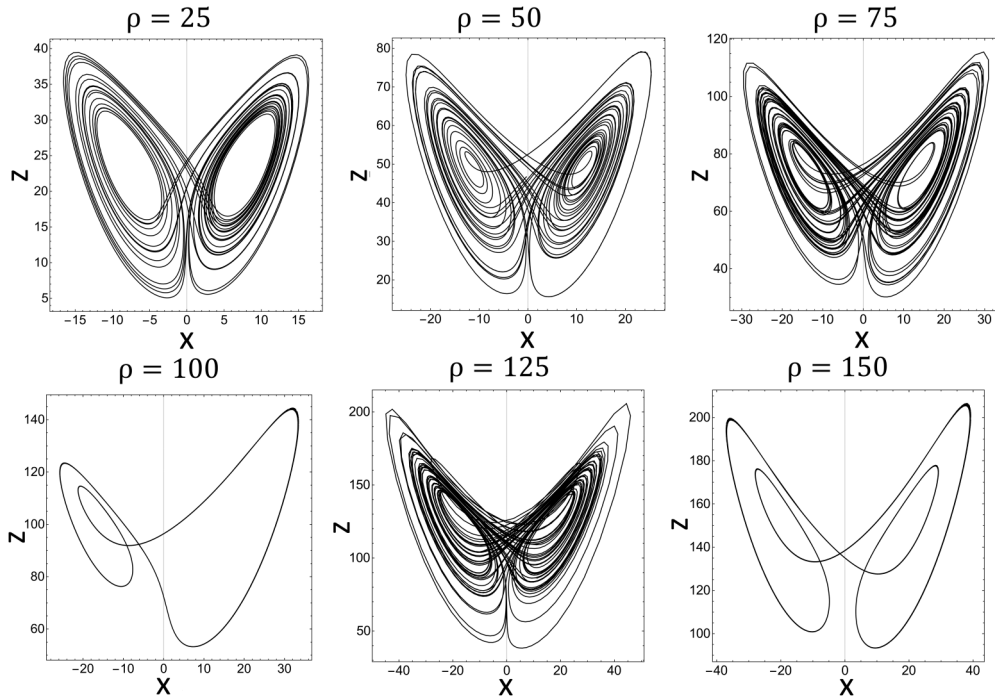


FIG. 4. Lorenz trajectories. Trajectories of the unmodified Lorenz system at different values of fixed ρ . Notice the quasiperiodic motion at $\rho = 100$ and $\rho = 150$. These are x - z projections of the full three-dimensional system. $\sigma = 10$, $\beta = 8/3$.

fluctuations in x as a function of (fixed) ρ . The average of x over 100 time units starting from different initial conditions, as a function of ρ , is shown in Fig. 6. Although the mean of x over a long time for any one value of ρ is zero, the spread of x averaged over an intermediate timescale varies. A period doubling window is responsible for the small-amplitude fluctuations shown in Fig. 6 near $\rho = 100$. As ρ approaches the top of this period doubling window the system spends fewer orbits going around one stationary point before switching to the other, causing the average x over intermediate time to be closer to 0. In the modified model, this spread plays the role of a state-dependent noise intensity which drives ρ . Comparison with Fig. 5 confirms that ρ gets hung up around places of low fluctuations in x before continuing to diffuse. Note that these correspond to regimes where there are stable periodic orbits in

the unmodified Lorenz equations. To highlight this point, we have indicated these regimes by horizontal red lines in both Fig. 5 and Fig. 6. There is also a somewhat weaker stall near $\rho \sim 130$. While this does not correspond to a period doubling window, Fig. 6 shows that this is nonetheless a region of low fluctuations.

In summary, the modified Lorenz system provides an illustrative example of a system with multiple possible behaviors that are manifested on an intermediate timescale and effectively slaved to the value of a slow variable, which in turn shows intermittent evolution due to feedback with the fast “fluctuating” degrees of freedom. Even though this is a perfectly deterministic system, ρ acts qualitatively like a variable that has an average drift down a gradient of fluctuation intensity that stalls in places of low fluctuation amplitude until there is a large enough kick to escape those areas.

IV. DISCUSSION

The short sequence of examples presented in this paper, taken together, represents a systematic progression in complexity, from many degree of freedom quasiperiodic, to a few degrees of freedom chaotic, to a single degree of freedom stochastic. The fundamental ingredients common to these examples are the decomposition into fast and slow subsystems along with two-way feedback between them. While ultimately our primary interest is in the deterministic many degrees of freedom case, the reduced stochastic model may prove more tractable. Suppose the collection of trajectories representing the dynamics of such a system can be coarse grained into multiple distinct possible behaviors and the amplitude of effective noise is large enough to drive the dynamics between different macroscopic patterns. The system spends irregular

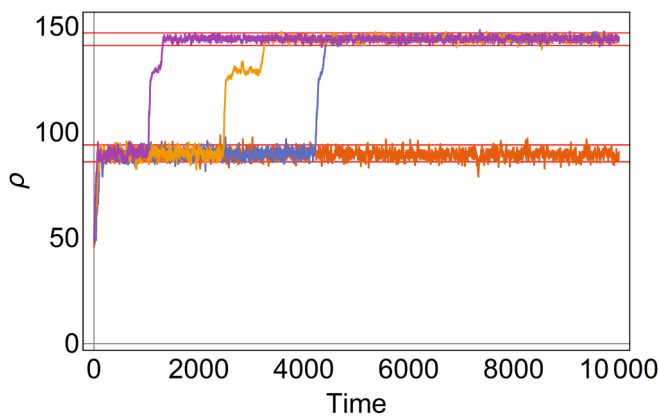


FIG. 5. Typical ρ time series. A collection of four ρ trajectories evolving according to Eqs. (3)–(6). The ranges highlighted by horizontal red lines are the same as in Fig. 6.

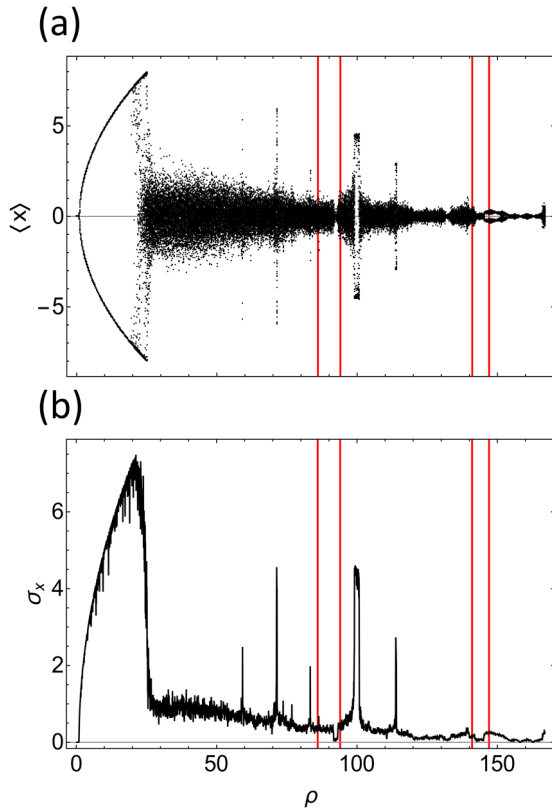


FIG. 6. Fluctuations in x . The fluctuations in x in the unmodified Lorenz system for different (fixed) ρ values. Places with very low fluctuations correspond to period doubling windows where the trajectories become periodic. (a) A plot of the average value of x for fixed ρ over 100 time units after a short transient from random initial conditions. (b) The standard deviation of x as a function of ρ .

intervals of time exhibiting one pattern before switching to another. Crucially, the system dwells longer in patterns in which the exhibited fluctuations are smaller. These features are not independent: they are two sides of the same coin. This becomes clear upon considering a limiting case: if one of the patterned behaviors is exactly periodic, the effective fluctuations are zero and the system will persist in that pattern indefinitely. This is just what happens in the metronome array for a sufficiently narrow frequency distribution [13,14]. Similarly, for a pattern that is only nearly periodic, the system dwells for a long but finite time before drifting into a new pattern.

An interesting recent experimental system that can be understood within this framework is the melting and refreezing of plasma dust “crystals” [17]. In this system, micron-scale particles are levitated in argon plasma above a negatively charged aluminum plate. Over a certain range of pressure and voltage a bistable dynamics is observed where the system switches between an orderly two-dimensional crystalline state and a disorderly gaslike state where the particles move erratically. The microscopic mechanical mechanism that triggers melting involves initially small oscillations of isolated particles in the plane perpendicular to the crystalline lattice [18]. Because the particles are not quite identical, they oscillate at slightly different frequencies. These differing fre-

quencies eventually lead to breaking of the lattice structure and the onset of an erratic and sustained gaslike state. Gradual damping results in kinetic energy loss and the eventual return to the crystalline state, and the cycle repeats, continuing indefinitely [17]. This is reminiscent of the metronome system discussed above, where there is a dynamically favored low-entropy state, but the disorder introduced by the nonuniform elements intermittently drives the system out of the highly ordered state.

A. A Reduced Model

The two above examples represent a class of deterministic systems that are sufficiently complicated that it makes sense to describe their behavior in terms of regular dynamical patterns with some effective noise. The statistical nature of the two examples can be treated similarly even though their complexity arises from different sources. In the case of the metronome system, the source of effective noise comes from the quenched distribution of natural frequencies being too wide to allow total synchronization. In the case of the modified Lorenz system, the effective noise arises from trajectories quickly spreading throughout the relevant attractor. In this section, we introduce a reduced model in which these elemental aspects are made explicit, namely, deterministic macroscopic behavior, a noise amplitude landscape, and mutual coupling between them. Specifically, we consider a stereotypic example of a mechanical particle moving in one dimension in a symmetric double-well potential, subject to dissipation and noise. The governing equation of motion is

$$\ddot{x} = ax(-x^2 + \gamma) + b\xi - c\dot{x}, \quad (7)$$

where x is the particle position, a , c , and γ are positive constants, ξ is Gaussian white noise with autocorrelation function $\delta(t_1 - t_2)$, and the noise amplitude b can be a function of x . Without noise ($b = 0$), the particle settles into one of the potential minima, its final state depending on its initial position and velocity. For constant noise amplitude ($b > 0$) the noise can drive the particle between the wells, on average spending equal time in each [Fig. 7(a)]. If instead the noise amplitude is dependent on the position of the particle such that the amplitude of noise is smaller in one of the wells than the other, then the particle spends most of its time in the well with lower noise, making only short excursions into the other [Fig. 7(b)]. To demonstrate this scenario we use a quadratic dependence with the minimum at the left well. This makes explicit the situation where there are two distinct states for the system created by the deterministic dynamics that are differentiated by noise amplitude. This is analogous to the situation in the metronome system above, for example, where there are two different possible behaviors for the system with one having lower effective noise. If the system operates in an intermediate regime—in which the noise is neither very weak nor very strong, so that the noise and the potential are equally important—the system displays the same kind of behavior seen in the two earlier examples: episodic intermittency with a preference for lower-fluctuation states. The double-well system embodies the essential ingredients, eliminating system-specific details while reproducing the features of the intermediate-timescale dynamics.

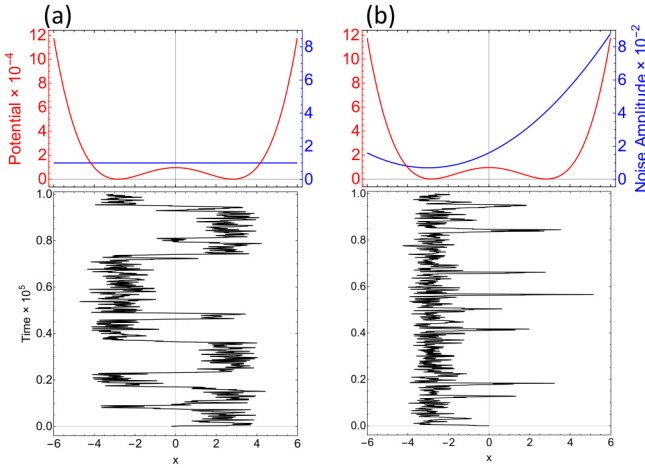


FIG. 7. Effect of noise gradient. The movement of a particle governed by Eq. (7). At the top, the deterministic potential is shown in red, and the noise amplitude b is shown in blue. At the bottom is the time series for x . The parameters for the deterministic potential in both cases are $a = 6 \times 10^{-6}$, $c = 0.01$, and $\gamma = 8$. (a) Time series for uniform noise amplitude ($b = 1 \times 10^{-2}$). The particle spends substantial time in each well before being kicked to the other. (b) Time series for nonuniform noise amplitude [$b = (x + \eta)^2 + \nu$ with $\eta = 3 \times 10^{-3}$ and $\nu = 7 \times 10^{-3}$]. The particle spends almost all of its time in the well with the lower amplitude noise, making only short excursions into the other well.

B. Rattling

Recently, the concept of “rattling” was proposed as a general organizing principle to account for the observation that some systems exhibit a preference for low effective-noise behaviors [9,10]. Specifically, the degree of rattling is a scalar measure which quantifies the long-term probability of a system spending time in a particular region of phase space by measuring the propensity of trajectories to exit that region. The claim is that if certain regions in phase space have a higher “effective temperature,” then trajectories will be quickly expelled from those regions and the system will spend less time in those regions on average. It is natural to ask whether, and to what extent, rattling may be relevant to the type of dynamics we have focused on in this paper. To this end, we have applied the definition of rattling provided in Ref. [10] to the modified Lorenz system.

The central prediction associated with rattling is that the probability of finding a system in a certain region of phase space is inversely related to the level of rattling in that region: that is, systems preferentially dwell in dynamical states of low rattling. In order to test this prediction, the rattling R and the long-term steady-state probability distribution p_{ss} must be calculated separately and compared. Both of these objects are scalar measures over the phase space of the system, and if the rattling hypothesis holds, then regions of lower R should be associated with regions of higher p_{ss} . The estimations of R and p_{ss} used here are based on the algorithm given in Ref. [10]. We run the system through 100 long (to $t_{\text{final}} = 1 \times 10^6$) integrations starting at random initial conditions. Then we cut these trials into shorter time windows of $\Delta t = 1$ to obtain a set of u_{it} where $u_1 = x$, $u_2 = y$, $u_3 = z$, and $u_4 = \rho$. Then we cal-

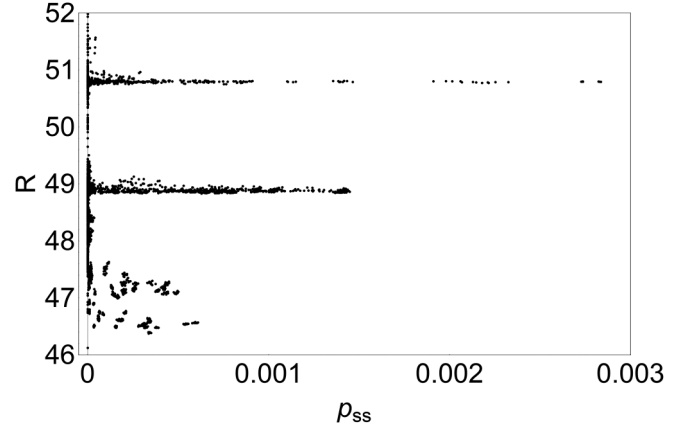


FIG. 8. Rattling vs steady-state probability. Each point represents the average rattling R over a region of phase space against the probability p_{ss} of finding the system in that region. Shown are a total of 9238 points, each representing one cube of phase space, out of a possible 20 736 after removing the cubes that the system did not enter.

culate the matrix $M_{ijt} = \frac{1}{\Delta t} (u_{i(t+\Delta t)} - u_{it})(u_{j(t+\Delta t)} - u_{jt})$. We obtain R with $R_t = \frac{1}{2} \ln[\text{Det}(M_{ijt})]$. Separately, we obtain p_{ss} by partitioning phase space into 12^4 cubes with side length 50 from -300 to 300 in each of the four variables. We then count the number of u_{it} in each cube, and normalize by the total number of u_{it} . To associate each phase space cube with an R value we average the values of R_t within each cube. Applying this algorithm to the modified Lorenz system [Eqs. (3)–(6)] yields Fig. 8. The features in Fig. 8 can be identified with corresponding system behavior. The two stripes at rattling values near $R = 49$ and $R = 51$ are the low fluctuation patterns highlighted in Fig. 5 and Fig. 6. The cloud of points below those stripes near $R = 47$ are the periodic trajectories found at very high values of ρ . These periodic trajectories are accessible only if the system is initialized at an already high ρ value. Similarly, in the lower left corner of Fig. 8 there is an isolated point corresponding to a stable fixed point which is accessible only if the system is initialized with a low enough ρ value. In the intermediate range the system spends the vast majority of time in one of the two patterns represented by the stripes near $R = 49$ and $R = 51$. This suggests treating the intermediate regime as a two-state system, with state 1 having higher values of ρ and lower values of R , represented by the lower stripe, and state 2 with lower values of ρ and higher values of R , represented by the upper stripe. With only two “patterns,” the system is perhaps too simple to represent a good test of the low rattling principle. Nevertheless, we verify that this system is consistent with the principle: in total, it has an 82% relative probability to be in state 1 and an 18% relative probability to be in state 2.

In conclusion, we have identified a class of dynamical systems that intermittently exhibit regular behavior over intermediate timescales, due to the low effective noise amplitude of those patterns. The persistence of these states is not indefinite, due to irregularities introduced either by the large number of degrees of freedom or by chaotic dynamics. These systems can be understood through a statistical approach that accounts for the dynamical patterns of the system. Many disparate

nonequilibrium systems can be understood through this common lens, from ecologies [1,2], to condensed matter [3,4], to turbulence [5,6], to robotics [7,10], to dusty plasmas [17,18]. A reduced stochastic model preserves the main dynamical features of these systems and may provide a means for making concrete theoretical progress.

ACKNOWLEDGMENTS

We would like to thank Dr. P. Chvykov for useful discussion during early portions of this research. This research was funded in part by ARO MURI Award No. W911NF-19-1-0233.

-
- [1] N. Eldredge and S. J. Gould, Punctuated equilibria: An alternative to phyletic gradualism, in *Models in Paleobiology*, edited by T. J. M. Schopf (Freeman Cooper, San Francisco, 1972), pp. 82–115.
 - [2] S. J. Gould and N. Eldredge, Punctuated equilibria: The tempo and mode of evolution reconsidered, *Paleobiology* **3**, 115 (1977).
 - [3] S. Field, J. Witt, F. Nori, and X. Ling, Superconducting Vortex Avalanches, *Phys. Rev. Lett.* **74**, 1206 (1995).
 - [4] R. G. Mints and I. Papiashvili, Flux creep in type-II superconductors: The self-organized criticality approach, *Phys. Rev. B* **71**, 174509 (2005).
 - [5] A. K. M. F. Hussain, Coherent structures—Reality and myth, *Phys. Fluids* **26**, 2816 (1983).
 - [6] B. Ganapathisubramani, E. K. Longmire, and I. Marusic, Characteristics of vortex packets in turbulent boundary layers, *J. Fluid Mech.* **478**, 35 (2003).
 - [7] W. Savoie, T. A. Berrueta, Z. Jackson, A. Pervan, R. Warkentin, S. Li, T. D. Murphey, K. Wiesenfeld, and D. I. Goldman, A robot made of robots: Emergent transport and control of a smarticle ensemble, *Sci. Robot.* **4**, eaax4316 (2019).
 - [8] P. Chvykov, On typicality and adaptation in driven dynamical systems, Ph.D. thesis, Massachusetts Institute of Technology, Cambridge, MA, 2019.
 - [9] P. Chvykov and J. England, Least-rattling feedback from strong time-scale separation, *Phys. Rev. E* **97**, 032115 (2018).
 - [10] P. Chvykov, T. A. Berrueta, A. Vardhan, W. Savoie, A. Samland, T. D. Murphey, K. Wiesenfeld, D. I. Goldman, and J. L. England, Low rattling: A predictive principle for self-organization in active collectives, *Science* **371**, 90 (2021).
 - [11] P. Yves and P. Manneville, Intermittent transition to turbulence in dissipative dynamical systems, *Commun. Math. Phys.* **74**, 189 (1980).
 - [12] D. Mingzhou, Intermittency, in *Encyclopedia of Nonlinear Science*, edited by Alwyn Scott (Taylor & Francis Group, Philadelphia, 2005), pp. 463–465.
 - [13] Ikeguchi Laboratory, Synchronization of 100 metronomes, Youtube (2015), www.youtube.com/watch?v=suxu1bmPm2g.
 - [14] H. Ulrichs, A. Mann, and U. Parlitz, Synchronization and chaotic dynamics of coupled mechanical metronomes, *Chaos* **19**, 043120 (2009).
 - [15] E. N. Lorenz, Deterministic nonperiodic flow, *J. Atmos. Sci.* **20**, 130 (1963).
 - [16] C. Sparrow, *The Lorenz Equations: Bifurcations, Chaos, and Strange Attractors* (Springer-Verlag, New York, 1982).
 - [17] G. Gogia and J. C. Burton, Emergent Bistability and Switching in a Nonequilibrium Crystal, *Phys. Rev. Lett.* **119**, 178004 (2017).
 - [18] J. Méndez Harper, G. Gogia, B. Wu, Z. Laseter, and J. C. Burton, Origin of large-amplitude oscillations of dust particles in a plasma sheath, *Phys. Rev. Research* **2**, 033500 (2020).